



Charge transfer in copper oxide nanostructure

J. Robin, K. Kelvin*

Department of Materials Science, Université Catholique de Louvain, Brussels, Belgium

*) Email: kkel@uclouvain.be

Received 2/12/2022, Accepted, 24/2/2023, Published 15/4/2023

The deposition potential affects the structural, morphological, optical, and electrochemical impedance spectroscopy properties of cuprous oxide (Cu₂O) thin films formed on copper (Cu) substrates adopting a three-electrode electrochemical deposition procedure. XRD data revealed that the deposited films have a cubic structure established with desired (111) growth orientation. Scanning electron microscopy (SEM) images reveal that Cu₂O film has very well three-sided pyramid-shaped grains which are equally spread over the surface of the Cu substrates and change substantially when the plating potential is changed. The photo-current density of prepared Cu₂O thin films was increased from -1.41×10^{-4} to -3.01×10^{-4} A/cm² with increasing the deposition potential of -0.3 to -0.6V, respectively. Further, Cu₂O thin films obtained at -0.6V have the minimum charge transfer resistance (R_{ct}) than Cu₂O thin films synthesized at -0.3 to -0.5V, suggesting that Cu₂O thin films produced at -0.6V have the highest electron transfer efficiency.

Keywords: Electrochemical deposition; Cuprous oxide; Nanostructure.

1. INTRODUCTION

In recent years, researchers have been drawn to semiconductor materials due to their wide range of applications in different fields. Because of their outstanding p-type semiconducting characteristics, cuprous oxide (Cu₂O) thin films are frequently used [1]. Almost every basic of present science and technology has been impacted by recent developments in nanomaterials. Controlling a material's structure, size, and morphology at the nano/microscale leads to better

controlling of its features and increased usability for a target case. Among the numerous metal oxide resources, cuprous oxide (Cu_2O) semiconductors are a particularly interesting research topic for a variety of disciplines [2]. Furthermore, it provides great charge transport and carriers concentrations enhancing the device efficiency. Chemical resistance, non-poisonousness, as well as abundance are additional benefits of this materials making it interesting also for solar cell applications [3]. Because it is a readily obtainable low-cost material, it has helped to realize low-cost photovoltaic technologies. Copper oxide occurs primarily in two forms, copper (I) oxide (Cu_2O) as well as copper (II) oxides (CuO). Those two components, having monoclinic and cubic structures, have straight band gaps ranging from 1.2→2.1 as well as 2.1→2.6 eV, respectively [4]. Because of having excellent optical and electronic characteristics, those two components have achieved widespread use in lithium-ion batteries, supercapacitors, gas sensing, and magnetically storing, as well as absorber layers in solar cells. It has gained interest as a result of its ubiquitous availability, protection of the environment, inexpensive prices, and suitability with a wide range of substrates [5]. Cu_2O has been generated to use a variety of processes, including sputtering, advanced oxidation processes, thermal decomposition, electrochemical deposition (ECD), and chemical vapour deposition (CVD). When comparing electrodeposition to other semiconductor growing techniques, this technology provides assets as well as advantages. This attraction stems from its ease of use, portability, and constructability, as well as its cheap cost deposition process which can be performed under standard lab conditions [6].

Over the previous few years, several attempts have been made to improve the precipitation of copper (I) oxide thin films with various features such as shape, size, and architecture through electro-chemical deposition (ECD), which has generated a lot of interest. Because remarkable features may be attained, Cu_2O can be adjusted into cubes [7], truncated, octahedral, faceted, polyhedral and flowerlike. By concentrating on the production of Cu_2O films via electrodeposition approach, researchers started to regulate the shape of formed thin films based on the applied voltage, ingredients, temperatures and pH, concentrations and electrolytes. There are limited research results exploring the influence of various applied potentials to the conductive electrode on which the Copper (i) oxide is electro-plated. Cu_2O was electrodeposited on different substrates and studied the growth of crystal and their effects on Photo-electrochemical characteristics [8]. Variation in Electrodeposition potential and current change the shape, size, morphology and orientation of thin films which may result variation in geometrical, optical, electrical and photo-conductivity properties. Moreover, the conductivity of Cu_2O films can be varied by changing the potential and pH of solution and in resultant photovoltaic parameters enhanced [9].

According to the above-mentioned literature studies, the majority of studies have concentrated on the impact of depositing voltages on crystal superiority, surface chemistry, electrolysis experiment, Eg, optical characteristics, and electrochemical impedance spectroscopy (EIS) of Cu_2O films. In the recent work, we focused on the improvement of the crystallographic Cu_2O films on copper (Cu) substrates under strong ac conductivity and photo-conductivity output using a 50°C temperature electro-deposition methodology over varied plating potentials ranging from -0.3 to -0.6V. We used alkaline solution which contains 0.4M copper sulphate (CuSO_4), 3M lactic acid and 4M sodium hydroxide (NaOH). The impact of varied plating potentials such as -0.3 to -0.6 V upon the structure, morphology, optical, and electrochemical impedance characteristics of

prepared Cu₂O thin films were characterized using X-ray diffraction (XRD), scanning electron microscopy (SEM), UV-vis spectroscopy, and electrochemical impedance spectroscopy (EIS), respectively [10].

2. EXPERIMENTAL

Copper sulphate (CuSO₄, 99% purity), lactic acid (CH₃CHCOOH, >98% purity), and sodium hydroxide (NaOH, required to regulate the pH value of the solution, 99% purity) were acquired through Sigma Aldrich as well as utilized exactly as directed. All the solutions used in this research were made within distilled water. Utilizing a 3-electrode cell configuration as shown in Figure 1, we have successfully electroplated Cu₂O thin films on copper (Cu) substrates with a surface area of 15 x 15 mm with a film thickness of 1 mm.

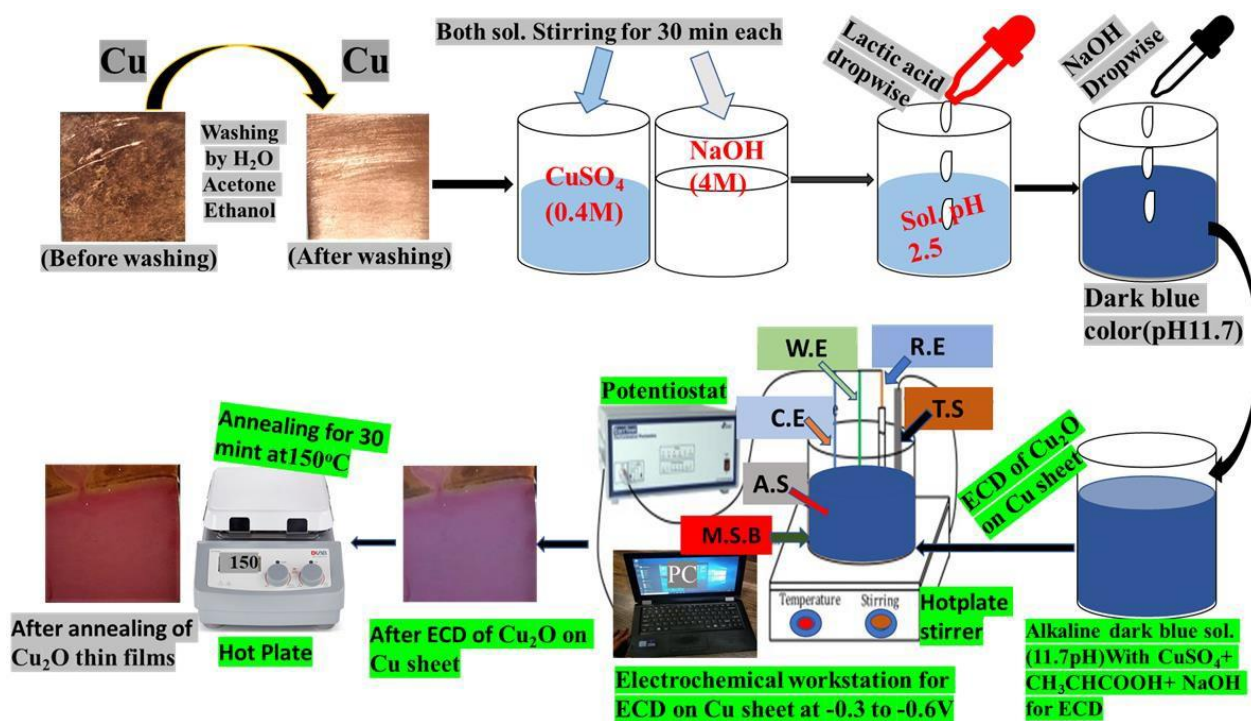


Figure 1 Schematic diagram for the deposition of Cu₂O thin films at a different applied potential.

Before the Cu₂O electrochemical deposition, the Cu substrates has been cleaned with acetone, isopropanol and distilled water in an ultrasonic bath for 10 minutes each. An electrochemical cell with a Cu substrate, platinum plate, and Ag/AgCl electrodes were mounted as a working electrode (W.E), a countering electrode (C.E), and a reference electrode (R.E), respectively. Copper sulphate water-less (0.4 M) and 3M lactic acid were used to prepare the deposition solutions, which were made individually and then mixed together for 30 minutes to achieve a homogeneous mixture. The lactic acid was used in the solution to maintain the Cu⁺² ions by complexing. The given reaction for the electrochemical plating of Cu₂O films over Cu substrates was done by the reduction of cupric lactate: $2\text{Cu}^{2+} + 2\text{e}^- + 2\text{OH}^- \rightarrow \text{Cu}_2\text{O} + \text{H}_2\text{O}$, this

reaction was expressed earlier. Drop by drop with a dropper, 4M NaOH solution was added to the mixture to adjust the pH to about 11.7. Utilizing the potentiostat (CS-350; Corrtest Instruments, Wuhan, China), the copper(i) oxide film was electroplated for 1200 (sec.) with changing plating potentials of -0.3 to -0.6 V against Ag/AgCl at a bath temperature of 50 °C. After that, the freshly prepared Cu₂O films were washed with distilled water as well as dried for half an hour at 150 °C in air.

The XRD curves of the generated films were captured via an X-ray spectrometer in the 2θ range of 20° to 80° (AXS D-8; Advance., Bruker, Germany), in which the X-ray emitter was a Cu Kα (K = 1.5406 Å, 40 kV, 200 mA). The morphology of synthesized materials was examined using a scanning electron microscope (Genesis-series, EmCRAFTSM, Korea). A Shimadzu UV- 2450 spectrophotometer was employed to express the optical characteristics of the produced films.

The fabricated films were measured by means of electrochemical impedance spectroscopy (EIS) in a sodium sulfate (Na₂SO₄) solution containing 0.5 mol/liter electrolyte. The (EIS) analysis was carried out by using three electrodes setup (CS-350; Corrtest Instruments, Wuhan, China) with a A.C amplitude of 10 mV and a frequency limit of 10⁻¹ to 10⁵ Hz. Typically, measurements were taken with the potentiostatic vs reference under consideration. At least three times, measurements were taken at room temperature. Finally, the capacitance measurements with AC amplitude of 10 mV and frequency of 3KHz were used to determine the conductivity type as well as carrier concentration of films.

3. RESULTS AND DISCUSSION

XRD analysis was accustomed to evaluate the crystal assembly and crystalline behavior of the electrodeposited Cu₂O films. Figure 2 describes the XRD symmetry of an electrodeposited thin film of Cu₂O on Cu substrate with several applied potentials from -0.3 to -0.6V. The cuprous oxide phase is confirmed by a sharp peak detected at 36.6° with the reflection plane of (111). All of the obtained diffraction peaks show that the sample is polycrystalline with a cubic structure, and the findings have good stability with the Joint Committee on Powder Diffraction Standards (JCPDS) card number 03-65-3288. The intensity of the (111) plane is enhanced by raising the applied potential from -0.3 to -0.6V, whereas the intensities of the other planes, namely (110), (200), (211), (220), (311) and (222), are drastically lowered. It demonstrates that the orientation improves along the (111) plane when potential levels rise from -0.3 to -0.6V. Based on such calculations, the crystallite size is raised from 39.46 to 47.52 nm by enhancing the deposition potential as the FWHM value decreases.

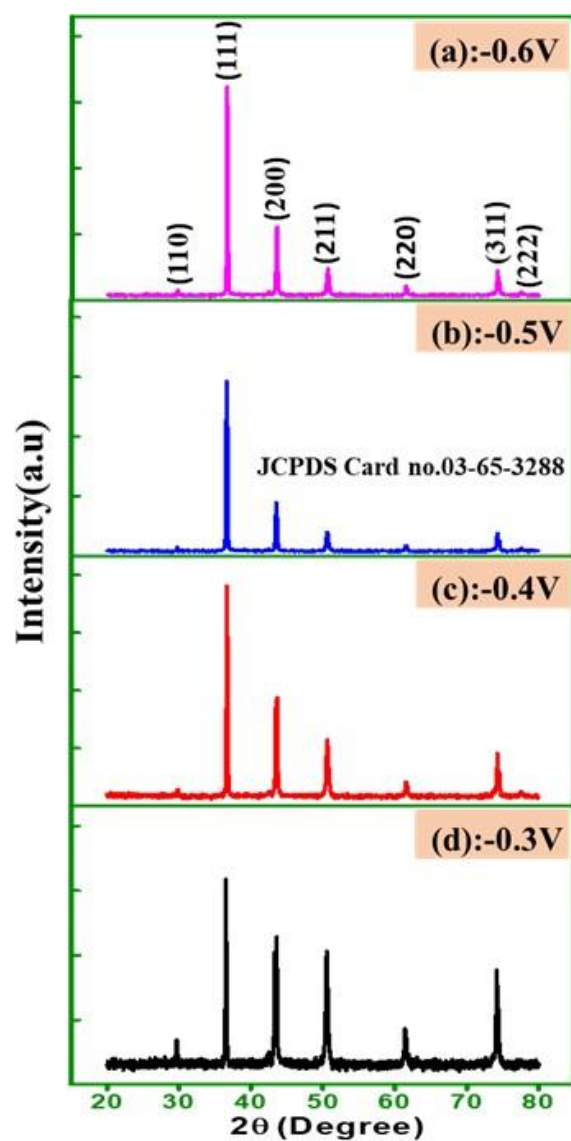


Figure 2 The XRD pattern of Cu₂O thin films prepared at a different applied potential.

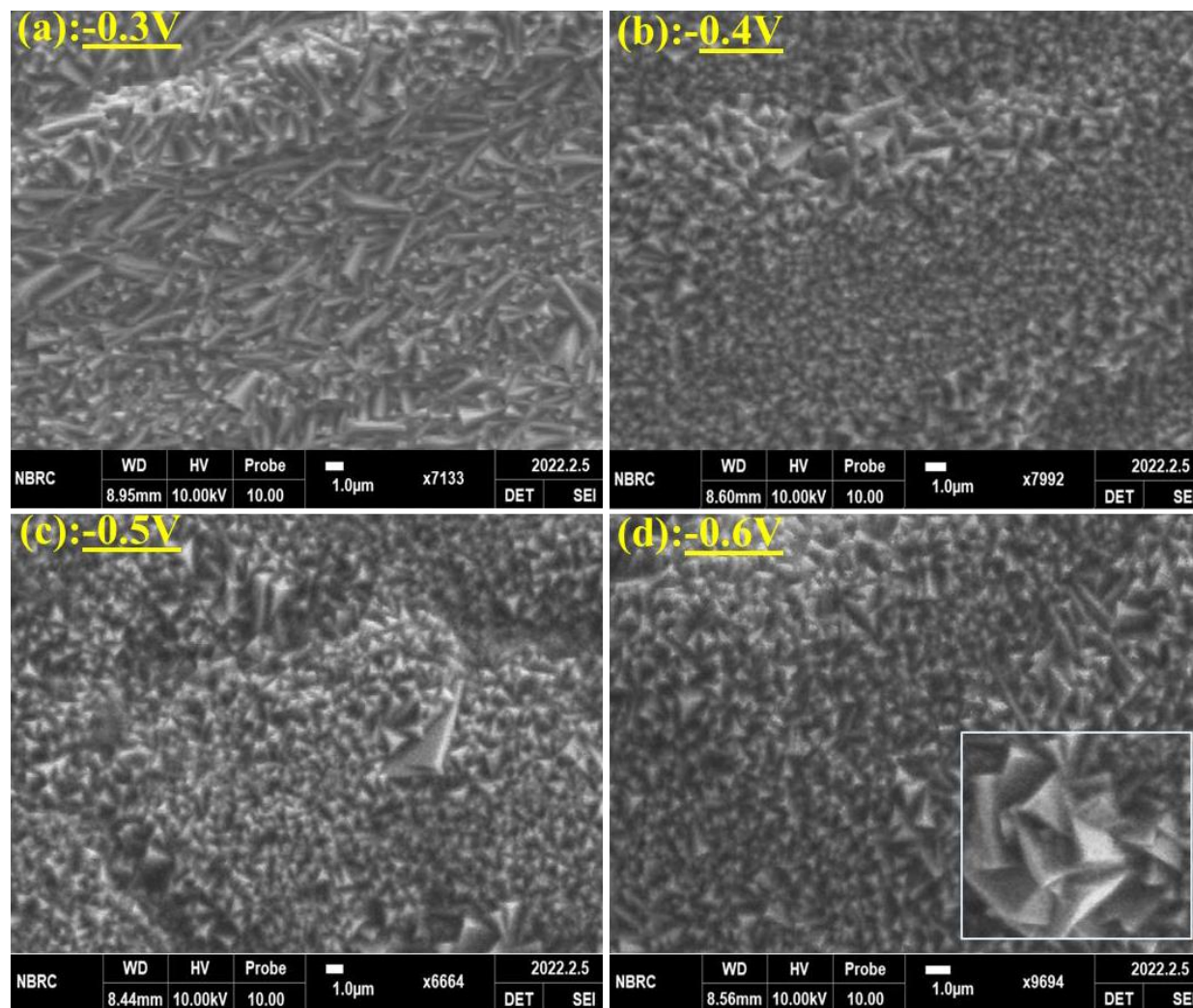


Figure 3 (a-d) The SEM images of prepared Cu₂O thin films on Cu substrate with different potential.

Scanning electron microscopy (SEM) is accustomed to analyzing the surface morphology of a material. SEM images of Cu₂O films produced over several plating potentials at -0.3 to -0.6V is illustrated in Figure 3. When the Cu₂O thin film is grown at a continuous overpotential of -0.3V, the 3-sided pyramid grain is consistently spread throughout the surface of Cu substrate without any voids, as illustrated in Figure 3(a). We observed from Figure 3(a), that there were some irregularities exist in the films because of the roughness of the Cu substrate. Furthermore, increasing the deposition potential to about -0.4V produces no morphological variations in 3-sided pyramid grains with decreasing the humps in the Cu₂O thin films, as seen in Figure 3(b), however, its size is significantly reduced. When such deposition potential is increased to -0.5V, 3-sided pyramid grains oriented in specific direction which is also clear from XRD results as illustrated in Figure 3(c). It can be estimated that when we enhanced the plating potential as of -0.3 to -0.4V, the size of 3-sided pyramid grains gradually decrease without any type of morphological change while the quantity of three-sided pyramid grains clearly increase as the deposition potential gets

more cathodic, due to a rise in Cu₂O crystal nucleation. Further, when we increase the deposition potential to -0.6 V, the morphology of Cu₂O thin film further changes from asymmetrical 3-sided pyramid grains into symmetrical grains without no voids and as illustrated in Figure 3(d). Earlier studies also described the formation of 3-sided pyramid surface morphology with Cu₂O films synthesized by an electrochemical deposition process. The current study indicates that the films produced at 0.6V have well oriented and thick three-sided pyramid-shaped grains, resulting in numerous reflections of an incoming photons. As a result, the films produced over - 0.6V are expected to be more stable and have improved optical behavior in optoelectronic applications.

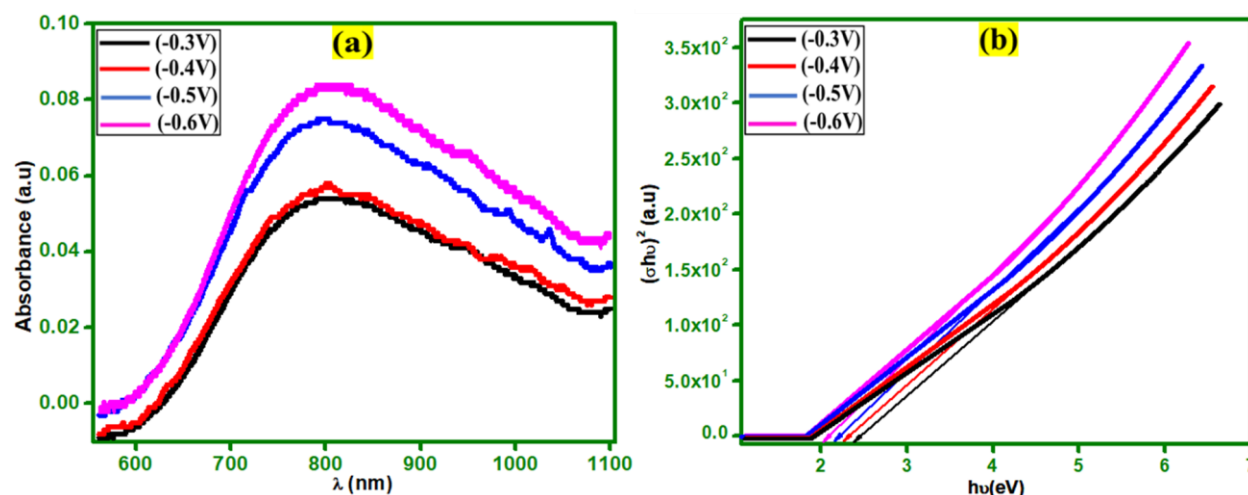


Figure 4(a-b) The absorbance and Tauc plot of Cu₂O films with various applied potential.

The absorption spectra of prepared Cu₂O thin films on Cu substrate were captured to find out the absorption coefficient and optical transition. The UV-visible absorption spectrum of Cu₂O films with a wavelength of 550 to 1000 nm is formed under various overpotentials as illustrated in Figure 4(a). In general, absorbance is affected by crystal assembly, morphology, surface quality, as well as film thickness. According to Figure 4(a), Cu₂O films produced over varying plating potentials have a distinct maximum absorption due to electron injection from valence channel to conduction channel. The optical absorbance of a Cu₂O film formed at -0.6V is higher than that of films synthesized at -0.3, -0.4, and -0.5V which we attribute to the symmetrical 3-sided pyramid denser grains. Because of the existence of a larger density with 3-side pyramid grains in films, the incoming light is multi-scattered at grain boundaries, allowing for increased photon absorption. According to observation that the absorbance edge of the film is red shifted from 785 to 830 nm as the plating voltage increased. The optical properties of Cu₂O like electron transition, optical band gap and absorption coefficients are evaluated by means of optical transmission and absorption.

The graph between $(\alpha h\nu)^2$ vs $(h\nu)$ was constructed for the determination of optical band gap as illustrated in Figure 4(b). The energy band gap (E_g) is calculated by extrapolating a linear mark intercepted above the X-axis. The thin films deposited at -0.3, -0.4, -0.5 and -0.6V result in band gaps of 2.35, 2.25, 2.15 and 2.01 eV, respectively. The optical band gap values of Cu₂O films produced by electro-deposition are comparable with earlier results. The band gap of Cu₂O films is reduced due to the factors such as crystallinity enhancement, morphological change and structural issues in films.

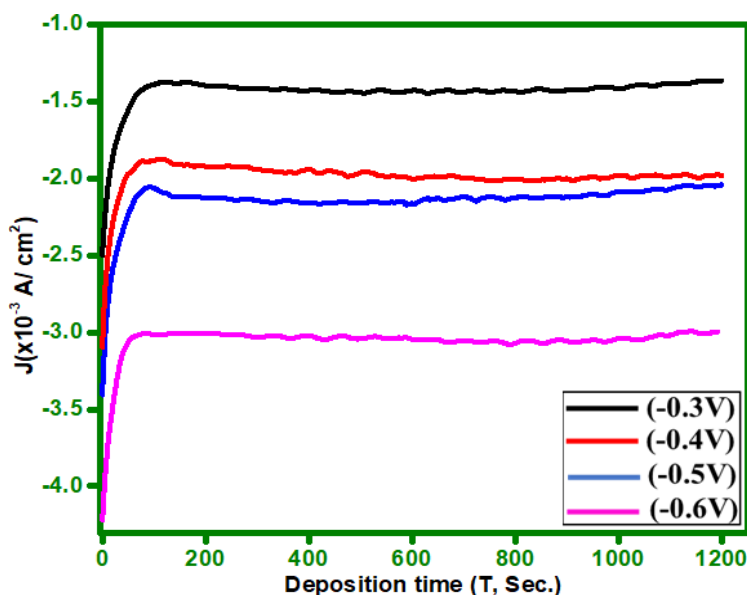


Figure 5 The current density plot of Cu₂O films prepared at a different applied potential.

The deposition time vs current density curves were obtained to evaluate the deposition speed during the electrodeposition procedure, as shown in Figure 5. The current density of an electroplated Cu₂O films on a Cu substrate under -0.6V was higher than that of Cu₂O obtained at 0.3, -0.4, and -0.5V, accordingly. This is evidently due to increased conduction, that allows the Cu substrate interface to be more efficient in reducing copper ions to generate the Cu₂O film. The current density of a Cu₂O layer at -0.6V on a Cu substrate regularly grew with period until it reached 100s, indicating that the Cu substrate surface was consistently covered by Cu₂O crystalline throughout the installation. After 100 seconds of depositing, the current remains stable throughout deposition which, indicates that Cu₂O films were completely covered the Cu substrate surface and also higher stable current for higher applied potentials. Furthermore, the greater current density of Cu₂O film on Cu substrate under -0.6V suggests an increase in surface area during Cu₂O thin film synthesis. The comparably lower current for Cu₂O synthesized from -0.3 to -0.5V suggests the development of small Cu₂O crystals with less surface area when compared to Cu₂O formed with -0.6V. These observations satisfy the previous reports. All of the outcomes corroborated and validated the SEM as well as XRD findings.

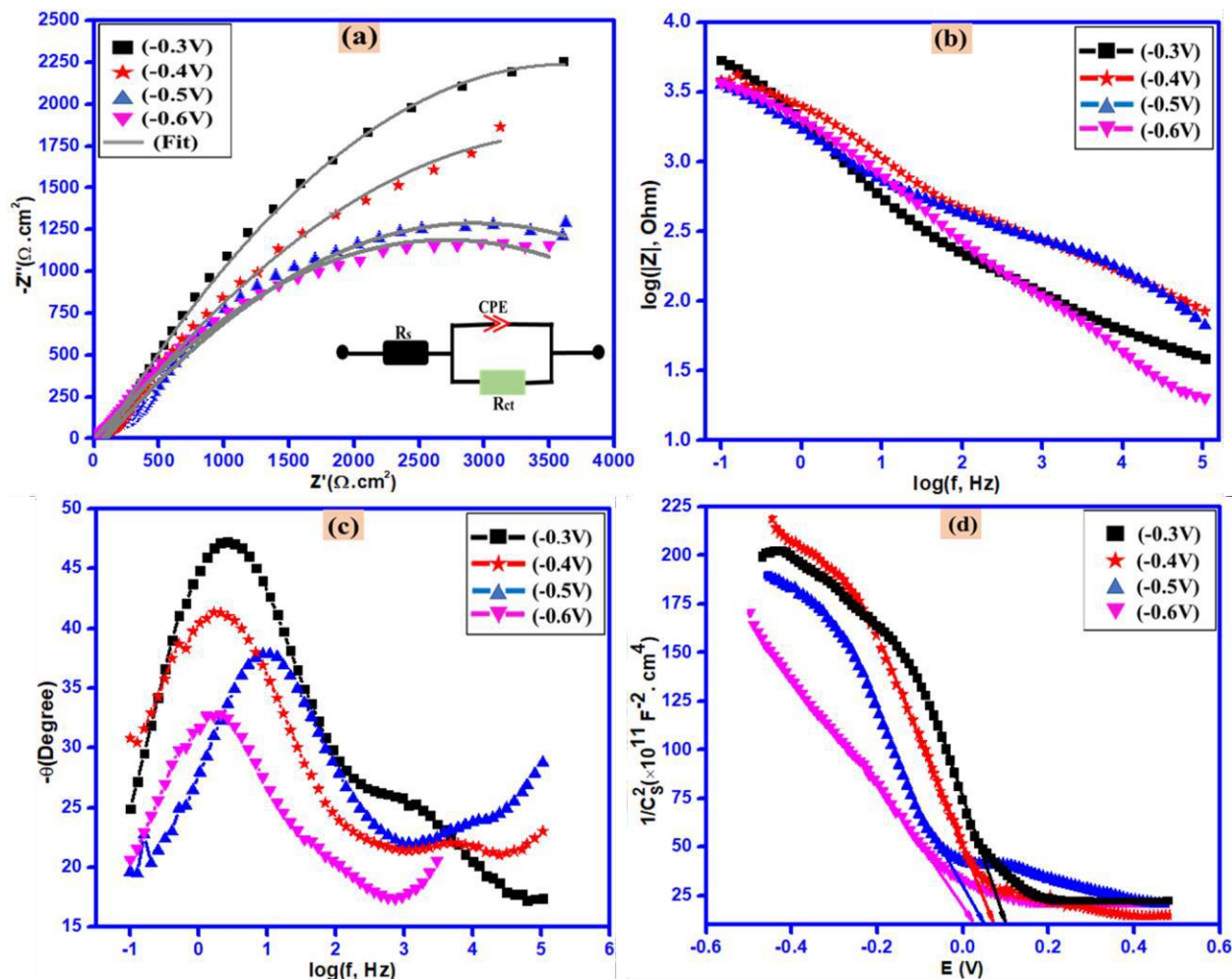


Figure 6 Nyquist plot with fitted equivalent circuit model, Bode plots and Mott-Schottky (M-S) plot for Cu₂O thin films prepared at different deposition potential; (a) Nyquist plots with fitted circuit model, (b) Bode modulus plots, (c) Bode phase plots and (d) Mott-Schottky (M-S) curve.

Figure 6(a) depicts the basic impedance spectra of Nyquist plot as real component (Z') vs imaginary component (Z'') with 0.5 M Na₂SO₄ solution for Cu₂O films produced over different coating voltages as -0.3 to -0.6V with an A.C frequency ranging from 10^5 to 10^{-1} Hz. We can observe from the Figure 6(a) that the Cu₂O electrodes' Nyquist plot shows throughout the higher-frequency domain semicircle arcs followed by an inclined line inside the low-frequency domain. In Nyquist plots, the dimension of the semicircle represents the resistance of charge transfer (R_{ct}). It can be used to define the electrode's interfacial features. As illustrated with Figure 6(a), when the plating potential is increased from -0.3 to -0.6V, then the diameter of semicircle of Cu₂O films clearly decreases. The drop-in electron passage barrier might be attributed to a kinetic barrier of electron carriage, which significantly interrupted interstitial electron transport upon the surface of electrode. The above trend may be seen in Figure 6(b), the cell was analyzed by utilizing the (EIS) measurement in the frequency range from 10^5 to 10^{-1} Hz over a

perturbed voltage of 10 mV in terms of bode modulus plot. The results of the electrochemical impedance spectroscopy (EIS) observations in this investigation are depicted in Figure 6(b), which includes the bode plot $\log|Z|$ vs $\log(f)$. As illustrated in exhibits Figure 6(b), the inclinations of four Bode plots $\log|Z|$ vs $\log(f)$ with applied potential under -0.3 to -0.6V are less than unity, suggesting pseudo-capacitive behavior. The above trend may be seen in the phase angle vs $\log(f)$ inside the bode phase diagram from Figure 6(c). There is only one phase angle crest visible, that is largest from 100→1000 Hz, demonstrating capacitive achievement within that frequency band. Because of frequency dispersal, the phase angle magnitude fluctuates from 55–70°, which is less -ve than the ideal capacitor of 90°C. We reported that thin films of cuprous oxide (Cu₂O) synthesized at -0.6V on a copper (Cu) substrate functioned better as a photo-absorber than thin films made at -0.3 to -0.5 V.

We can also see a modest trend in the direction of lesser frequencies, that might be due to increased carrier motion lowering charge transfer resistance. Taking the EIS spectra into consideration, it became feasible to simulate the interfacial junction using a Randles comparable circuit model in Z View 3.0, when we see inside of Figure 6(a). As we have seen that the experimental and simulated results are very similar. In all situations, the calculated variables' standard deviations are under 5%, indicating a satisfactory fitting. The charge transfer resistance (R_{ct}), resistance of electrolyte solution (R_s), as well as constant phase element (CPE) are all part of the circuit. The CPE is primarily used to describe non-homogeneity in a system as well as the spreading of physical system software attributes. Throughout the whole deposition potential range of -0.3 to -0.6V, the electrolyte resistance R_s solution stays constant, with estimates ranging from 37.86 to 11.27 Ω.cm². The rise in the depositing potentials of Cu₂O films results in a substantial decrement in charge transfer resistance (R_{ct}) under 9.2×10⁴ to 6.4×10³ Ω .cm². And the CPE is also decreased in the vicinity of 2.3×10⁻⁴ to 1.6×10⁻⁴ F. cm⁻². The quick charge transmission within Cu₂O films as electrode as well as the large electrons density over the interstitial afterwards raising the plating potential from -0.3 to -0.6V or the film depth might explain this phenomenon. This might be attributed to the lower grain size and a reduction in grain boundaries. The Mott-Schottky (M-S) method was accustomed to determine the doping type, as well as the flat band potential (E_{fb}) was calculated by means of intercept on the voltage axis as 1/C²=0. Boltzmann constant, absolute temperature and the acceptor concentration, respectively. Mott-Schottky plot reveals the semiconductor's conductivity nature, with a -ve sign for p- type and +ve for n-type semiconductors. Figure 6(d) shows the Mott-Schottky graphs obtained from Cu₂O produced at various coating potentials in 0.5M Na₂SO₄ under a frequency of 3kHz. A linear correlation between 1/C² and E may be seen by using the Mott-Schottky formula. The negative inclinations show the whole samples are a p-type semiconductor that carry holes among Cu₂O having a value of ε was 6.3. We further noticed that by raising the plating voltage over -0.3→-0.6 V, the flat-band potential (V_{fb}) changes dramatically under 0.132 to 0.108 eV against Ag/AgCl. This can be attributed to variation in morphology as well as crystal assembly that occurs whenever depth of the film is increased. The acceptor concentration is calculated by means of slopes acquired from an inspection of Mott-Schottky graph. Our findings are in well agreement with those of other researchers who have discovered a distinctive value of 10¹⁵→10¹⁸ cm⁻³ for Cu₂O thin films.

4. CONCLUSIONS

In this article, p-type Cu₂O thin films were synthesized by electrochemical deposition employing three electrodes system in an alkaline electrolytic solution with pH 11.7 comprising 0.4M (CuSO₄), 3M (CH₃CHCOOH), and 4M (NaOH). We inspected the production of Cu₂O films through electroplating by applying the alternative applied potentials to the working electrodes and reported that potential selection has a significant role in influencing the development of the Cu₂O films in absence of additives or buffers. XRD peaks indicated that the films produced at -0.6V have cubic structure and excellent crystallinity with the associated (111) plane. Scanning electron microscopy (SEM) pictures revealed that the Cu₂O films produced over -0.6V have 3-sided pyramid dense grains spread out uniformly on the surface of Cu substrate. UV- visible investigation demonstrates that the absorbance of a Cu₂O thin film coated under -0.6V is significantly greater than that of other films formed at -0.3 to -0.5V. The band gap (E_g) of Cu₂O films decreases from 2.35 to 2.01 eV when the plating voltage rises from -0.3 to -0.6V.

References

- [1] T. Wong, S. Zhuk, S. Masudy-Panah, and G. Dalapati, *Materials* 9 (2016) 271
- [2] T. Mahalingam, J. S. P. Chitra, J. P. Chu, H. Moon, H. J. Kwon, Y. D. Kim, *J. Mater. Sci. Mater. Electron.* 17 (2006) 519
- [3] M. A. Hossain et al., *Mater. Sci. Semicond. Process.* 63 (2017) 203
- [4] S. Santhosh Kumar Jacob et al., *Mater. Res. Express* 6 (2019) 046405
- [5] R. David Prabu, S. Valanarasu, V. Ganesh, M. Shkir, A. Kathalingam, S. AlFaify, *Surf. Coatings Technol.* 347 (2018) 164
- [6] F. Vervliet, D. Willinger, L. C. Alvarez, *Exp. Theo. NANOTECHNOLOGY* 5 (2021) 169
- [7] Alfarooq O. Basheer, S. Abdullah, V. K. Arora, *Exp. Theo. NANOTECHNOLOGY* 5 (2021) 175
- [8] A. Subhi, M. A. Saeed, *Exp. Theo. NANOTECHNOLOGY* 5 (2021) 181
- [9] K. Han and M. Tao, *Sol. Energy Mater. Sol. Cells* 93 (2009) 153
- [10] Y. Wang, L. Liu, Y. Cai, J. Chen, J. Yao, *Appl. Surf. Sci.* 270 (2013) 245

